



Preparation and characterization of PVDF–PVP–TiO₂ composite hollow fiber membranes for oily wastewater treatment using submerged membrane system

C.S. Ong^{a,b}, W.J. Lau^{a,b,*}, P.S. Goh^{a,b}, B.C. Ng^{a,b}, A.F. Ismail^{a,b}

^aAdvanced Membrane Technology Research Centre (AMTEC), Universiti Teknologi Malaysia, Skudai, Johor 81310, Malaysia

^bFaculty of Petroleum and Renewable Energy Engineering, Universiti Teknologi Malaysia, Skudai, Johor 81310, Malaysia
Tel. +60 75535926; emails: lwoeijye@utm.my, lau_woeijye@yahoo.com

Received 14 August 2013; Accepted 1 October 2013

ABSTRACT

A series of polyvinylidene fluoride (PVDF) hollow fiber ultrafiltration membranes made of different titanium dioxide (TiO₂) concentrations with the presence of polyvinylpyrrolidone as additive was prepared. The membrane performances were characterized in terms of pure water flux, permeate flux, and oil rejection, while the membrane morphologies were analyzed using scanning electron microscope and atomic force microscope. The experimental results showed that when 2 wt.% TiO₂ was incorporated into PVDF membranes, optimized permeate flux and oil rejection of 70.48 L/m²h (±1.41) and 99.7% (±0.3), respectively, could be obtained when tested using 250 ppm synthesized oily solution under vacuum condition. Compared to the PVDF membrane without TiO₂ addition, all the composite membranes showed relatively higher permeate flux and oil rejection. Based on the results obtained, it is reported that the composite PVDF membrane incorporated with 2 wt.% TiO₂ exhibited the best separation performance in which complete removal of oil was able to achieve regardless of the feed oil concentration. However, decrease in permeate flux was observed when the feed oil concentration increased from 250 to 1,000 ppm. The results concluded that the composite PVDF membrane showed better performance in treating oily solution compared to that of without TiO₂.

Keywords: Polyvinylidene fluoride; Ultrafiltration; Oily solution; Titanium dioxide; Hydrophilicity

1. Introduction

Nowadays, the global oil demand is increasing to an unprecedented high level owing to the rapid development of automobile industry and the high fuel consumption for industrial production. This as a consequence has resulted in large amount of oily

wastewater generated from oil refinery industry. As oily wastewater contains many hazardous hydrocarbon mixture, chemical components, and heavy metals, it is required to be treated before discharging to receiving water body. Currently used biological, chemical, and physical treatments are not efficient enough to completely separate oil molecules from water and generally require large space to construct, thus making them economically unviable [1–5]. To

*Corresponding author.

tackle this issue, membrane technology has been considered as a promising candidate to replace the existing technologies to treat oily wastewater [3,5–8]. The significant advantages of using ultrafiltration (UF) membrane for this oily wastewater treatment process are: high efficiency in removing oil droplets, low energy consumption, minimum chemicals used (only for cleaning process), and no production of by-product. Nevertheless, the application of UF membrane is also hindered by some undesirable drawbacks. Particularly, the membrane water flux deterioration is always associated with fouling problem that resulted from the absorption and accumulation of oil particles on the membrane surface [9].

To tackle this problem, antifouling and hydrophilic additives are incorporated into polymeric membranes to enhance their fouling resistance. Although polyvinylidene fluoride (PVDF) is one of the several main polymer materials used in making UF membranes, its hydrophobic nature is commonly related to low water permeability and high fouling tendency, particularly when the membrane is used to remove hydrophobic oil molecules [8]. In order to increase membrane hydrophilicity and fouling resistance, titanium dioxide (TiO_2), lithium chloride, polyvinylpyrrolidone (PVP), and polyethylene glycol have been widely used as hydrophilic additives for PVDF membrane fabrication. Yuan and Li [10] found that PVP with molecular weight ranging from 25,000 to 40,000 Da could act as phase demixing enhancer and further improve the membrane porosity and permeability. Xu et al. [11] studied the effect of PVP with molecular weights ranging from 10,000 to 1,300,000 Da on the morphological properties of polyetherimide membrane. They found that larger pores were formed on membrane surface upon the addition of lower molecular weight of PVP (i.e. 10,000 and 40,000 Da), thus leading to greater water permeability. Chakrabarty et al. [9] also reported that the membrane flux was able to improve with the use of lower molecular weight of PVP (ranging from 24,000 to 40,000 Da) due to the formation of larger pore sizes on the membrane surface.

In addition to polymeric additives, inorganic TiO_2 nanoparticles have also received attention among membrane scientists due to their capability to reduce membrane fouling tendency. Recent studies showed that the antifouling properties of TiO_2 -deposited membranes are higher than that of neat membranes [12–14]. According to Rahimpour et al. [15], membrane fouling can be mitigated by adding TiO_2 into PVDF membrane blended with sulfonated polyethersulfone (SPES). The total flux losses of TiO_2 deposited PVDF/SPES membrane were lower than the PVDF/SPES blended membrane. Damodar et al. [14] also reported

that good hydrophilicity of membrane was established by adding low concentration of TiO_2 into the PVDF casting solution. Oh et al. [13] modified PVDF–UF membrane with TiO_2 nanoparticles and found that the fouling resistance of the composite PVDF membranes was significantly improved.

In view of the importance of adding hydrophilic additives in improving PVDF membrane properties, the main objectives of this study are to prepare and characterize PVDF-hollow fiber membranes blended with PVP incorporated with different concentrations of TiO_2 nanoparticles (ranging from 0 to 4 wt.%) for oily wastewater treatment under submerged conditions. The results obtained from this study demonstrated the potential of using PVDF composite membranes with enhanced hydrophilicity and low fouling tendency for treating industrial oily effluent.

2. Experimental

2.1. Materials

PVDF (Kynar[®]760) pellets purchased from Arkema Inc., Philadelphia, USA were used as the main membrane forming material. N,N-dimethylacetamide (DMAc) (Merck, > 99%) was used as solvent to dissolve polymer without further purification. PVP (K30) purchased from Fluka and TiO_2 (Degussa P25, average particle size ~21 nm) from Evonik were used as additives to enhance PVDF membrane properties. The cutting oil obtained from RIDGID, Ridge Tool Company was used to synthesize oily solution with different oil concentrations.

2.2. Preparation of membrane and membrane module

Eighteen weight percent of PVDF was added into pre-weighed DMAc solvent after being dried for 24 h in oven at 50 °C (± 1). The solution was then mechanically stirred at 600 rpm until all PVDF pellets were completely dissolved. It was followed by the addition of 5 wt.% PVP and certain amount of TiO_2 nanoparticles (ranging from 0 to 4 wt.%) to produce dope solutions with different TiO_2 concentrations. Lastly, the dope solution was ultrasonicated prior to spinning process to remove any air bubbles trapped within the solution.

Using the solutions prepared, PVDF membranes were fabricated using dry-jet wet spinning method as described elsewhere [16]. The details of spinning conditions are shown in Table 1. The as-spun hollow fibers were immersed into water bath for 2 days to remove residual solvent. Prior to air drying, the fibers were post-treated using 10 wt.% glycerol aqueous

solution for 1 day with the aim of minimizing fiber shrinkage and pore collapse. Finally, the hollow fiber membranes were dried at room temperature for 3 days before module fabrication.

A bundle of 60 hollow fibers with approximate length of 28 cm (total effective membrane area: 607 cm²) was potted into PVC tube using epoxy resin (E-30CL Loctite® Corporation, USA). The module was then left at room temperature for hardening before its protruding parts were cut and fixed into a PVC adaptor to complete the module preparation.

2.3. Preparation of synthetic oily solution

The synthetic oily solution was prepared by mixing distilled water with commercial cutting oil. The emulsion was prepared by keeping the oil-water mixture in a blender for several minutes at room temperature. The size of oil droplets was measured using Zetasizer Nano ZS (Malvern Instrument Inc., Southborough, MA), with refractive index of 1.47 and 1.333 for the oil droplets and dispersant (water), respectively. The oil droplet size distribution was in the range of 0.4–2.6 μm with an average particle diameter of 1.08 μm (±0.16), as shown in Fig. 1.

2.4. Filtration experiment

The separation performance of hollow fiber was assessed using a submerged system. To minimize the fouling effect, a constant air flow rate of 5 mL/min generated by an air compressor (2 HP single cylinder 24 L tank, Orimas) was used to generate air bubbles in the submerged tank through air diffuser installed under the tank. Water permeate was then produced using peristaltic pump (Model: 77200–60, Masterflex L/S, Cole Parmer) by creating vacuum condition on permeate side. The permeate was taken every 10 min

Table 1
Hollow fibers spinning conditions

Spinning parameters	Value
^a OD/ID of spinneret (mm/mm)	1.15/0.55
Dope flow rate (cm ³ /min)	10.5
Bore fluid rate (cm ³ /min)	3.5
Bore fluid temperature (°C)	27
Air gap distance (cm)	3
External coagulant	Tap water
Coagulant temperature (°C)	27
Wind-up drum speed (cm/s)	18.3

^aOD/ID = Outer diameter/inner diameter.

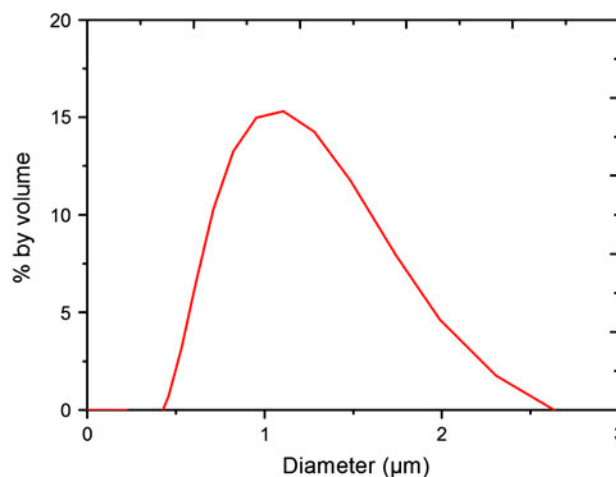


Fig. 1. Size distributions of oil droplets in synthetic oily solution (oil concentration = 250 ppm).

and the water flux (J) was determined according to Eq. (1).

$$J = \frac{Q}{At} \quad (1)$$

where J is the water flux (L/m²h), Q is the quantity of permeate (L), A is the effective membrane area (m²), and t is time to obtain the quantity of Q (h).

The membranes were tested using feed oil solution with concentration of 250, 500, and 1,000 ppm. The membrane oil rejection was then determined based on Eq. (2).

$$R = \left(1 - \frac{C_p}{C_F}\right) \times 100 \quad (2)$$

where R is the oil rejection (%), C_p and C_F are the concentration of the permeate (ppm) and the feed (ppm), respectively. The oil concentrations in permeate and feed were determined using UV-vis spectrophotometer (Model: DR5000, Hach) with absorbance measured at 294 nm, where the maximum absorption occurs.

2.5. Membrane characterization

2.5.1. Contact angle goniometer

The contact angle of membranes was determined by sessile drop technique using contact angle goniometer (Model: OCA 15EC, Dataphysics) with deionized water as the contact liquid. At least 10 locations on the membrane surface were arbitrarily measured and the results were reported as their average value.

2.5.2. Scanning electron microscope

The outer surface and cross sectional morphology of membranes was observed by scanning electron microscope (SEM) (Model: TM 3000, Hitachi). Prior to the analysis, the hollow fiber was immersed into liquid nitrogen for few minutes followed by freeze-fracturing to obtain perfect cut structure. The fiber was then placed onto carbon-tape aluminium holder and coated with gold under vacuum.

2.5.3. Atomic force microscope

The membrane surface roughness and mean pore sizes were investigated by atomic force microscope (AFM) (Model: SPA-300HV, Seiko). A small piece of fiber was cut and adhered on a 1 cm² square paper card using double-sided adhesive tape. The membrane surface was scanned in the size of 5 μm × 5 μm. The surface roughness of the membrane was expressed in terms of mean surface roughness (R_n). Pore size on membrane outer surface was measured by visual inspection on the obtained line profiles from AFM images of the same membrane at different areas. To obtain the pore size, cross-sectional line profiles were selected to traverse the micron scan surface areas of the AFM images. The pore diameter was measured by inspecting line profiles of different high peaks and low valleys on the same AFM images. The pore sizes were reported based on the average of 60 measurements.

In order to investigate the pore size distribution, 60 dark spots from the AFM images are measured and a graph was plotted according to the method described by Khayet et al. [17]. Based on this method, the measured pore sizes are arranged in an ascending order. Median ranks are calculated using Eq. (3).

$$\text{Median or 50\% rank} = \left[\frac{j - 0.3}{n + 0.4} \right] \times 100\% \quad (3)$$

where j is the order number of the pores when arranged in ascending order and n is the total number of pores measured.

If pore sizes have log-normal distribution, the median rank vs. ascending pore size would be a straight line on the plot graph. From the graph, the mean pore size (μ_p) and geometric standard deviation (σ_p) can be determined. The mean pore size will correspond to 50% of cumulative number

of pores and the geometric standard deviation can be calculated from the ratio of 84.13% of cumulative number of pores to that of 50%. From the mean pore sizes and geometric standard deviation, the pore size distribution can be determined by using Eq. (4).

$$\frac{df(d_p)}{d(d_p)} = \frac{1}{d_p \ln \sigma_p (2\pi)^{1/2}} \exp\left(-\frac{(\ln d_p - \ln \mu_p)^2}{2(\ln \sigma_p)^2}\right) \quad (4)$$

where d_p is membrane pore size (nm), σ_p is geometric standard deviation, and μ_p is mean pore size (nm).

2.5.4. X-ray diffraction

X-ray diffraction (XRD) patterns of the membranes were obtained with an X-ray diffractometer (D/max-rB 12 kW, Rigaku) equipped with Nickel (Ni)-filtered Copper (Cu) K α radiation ($\lambda = 1.54056 \text{ \AA}$) operated at 50 mA and 50 kV. The measurement was executed by monitoring the diffraction angle 2θ from 5 to 60° with a step increment of 0.05°.

2.5.5. Mechanical tensile test

The fiber tensile test was performed at room temperature on a tensile tester (Model: LRX2.5KN, LLYOD). The gauge length of membrane sample was fixed at 50 mm and the gauge running speed was set at 10 mm/min. The tensile strength and elongation-at-break of the membrane were then evaluated using NEXTGEN software.

2.5.6. Membrane porosity

The membrane porosity, ε , is defined as the volume of the pores per the total volume of the porous membrane as shown in Eq. (5).

$$\varepsilon = \frac{\frac{(w_{\text{wet}} - w_{\text{dry}})}{\rho_w}}{\frac{(w_{\text{wet}} - w_{\text{dry}})}{\rho_w} + \frac{w_{\text{dry}}}{\rho_p}} \times 100 \quad (5)$$

where ε is the membrane overall porosity (%), w_{wet} is the weight of wet membrane (g), w_{dry} is the weight of dry membrane (g), ρ_p is the density of the polymer (g/cm³), and ρ_w is the density of water (g/cm³).

3. Results and discussion

3.1. Effect of TiO₂ concentration on membrane structural properties

Table 2 summarizes PVDF–TiO₂ membrane properties with respect to their porosity, mechanical strength, contact angle, and pore size. It is generally reported that TiO₂ nanoparticles could significantly increase membrane porosity [12,18–21], but the improvement on membrane porosity was insignificant in this study as all the membranes prepared displayed reasonably high porosity, i.e. between 84.1 and 88.6%. It is thus believed that the presence of hydrophilic PVP with high MW has contributed greatly to high membrane porosity regardless of the TiO₂ concentration. According to Yuan and Li [10], the presence of PVP in dope solution could induce solution demixing during phase inversion and enhance the phase separation, hence resulting in the macropore enlargement which is related to high porosity. The membrane porosity was reported to be more than 80% with increasing PVP concentration from 1 to 5 wt.% in the dope solution [10], which is similar to the results reported in this study. With respect to mechanical strength, all PVDF membranes incorporated with TiO₂ nanoparticles demonstrated greater mechanical strength compared to that of without TiO₂. The noticeable trend is explained by the suitability of TiO₂ as an ideal filler for polymeric PVDF membrane due to its excellent mechanical properties, high surface area, and high aspect ratio. However, it has been previously reported that improved mechanical strength could only be obtained using an optimized loading of inorganic filler [22]. With respect to hydrophilicity, the contact angle decreased as the TiO₂ concentration increased from 1 to 2 wt.%, but gradually increased with further increase in TiO₂ concentration to 3 and 4 wt.%. When the concentration of TiO₂ was increased from 0 to 2 wt.%, the contact angle of PVDF membranes was reported to decrease due to the

enhanced surface hydrophilicity. However, when the concentration of TiO₂ was further increased up to 4 wt.%, the effect of surface roughness became dominant and decreased the surface hydrophilicity due to Cassie effect [23]. As a result, increased membrane contact angle was observed at high TiO₂ loading.

As observed in the SEM images (Fig. 2), the finger-like structure developed from the outer surface layer and became wider across the membrane cross-sectional area. No significant difference was observed in the cross-sectional structure of the PVDF membrane with and without the addition of TiO₂. However, the dispersion of TiO₂ on the membrane's top surface was observed upon the addition of TiO₂ from 1 to 4 wt.%. It was noticed that TiO₂ nanoparticles were dispersed across the surface of membranes made of 1 and 2 wt.% of TiO₂ but at higher concentration of TiO₂ (i.e. 3 and 4 wt.%), these nanoparticles tended to agglomerate and form bigger size of nanoparticles. Although the number of pores appeared more in the membrane with increasing TiO₂ concentration from 3 to 4 wt.%, the agglomerated TiO₂ nanoparticles would have blocked the pores, resulting in lower water flux.

Fig. 3 presents three-dimensional AFM images and surface roughness (R_a) of the PVDF membranes prepared at different TiO₂ concentration. The AFM images clearly indicated that membrane surface roughness was strongly dependent on the loading of TiO₂. It was observed that the R_a value of membrane increased from 10.4 to 31.7 nm with increasing concentration of TiO₂ from 0 to 4 wt.%, possibly ascribed to the nodular shapes of TiO₂ nanoparticles that have resulted in the development of ridge-and-valley structure on the membrane surface [25].

Fig. 4 shows the pore size distribution of PVDF membrane incorporated with different concentrations of TiO₂. With increasing concentration of TiO₂ from 0 to 4 wt.%, wider pore size distribution and larger pore size were observed. It was reported that the average pore size determined from SEM images are smaller than that of obtained from AFM topography probably due to the effect of metal coating. On the other hand, it is previously reported that the pore size measured by AFM is about three times larger than that of determined by solute separation [17,24,25]. Since the pore sizes of all the membranes were determined using AFM, it shows reasonably larger mean pore sizes, as illustrated in Table 2.

Fig. 5 presents the XRD patterns of PVDF–TiO₂ composite membranes and PVDF membrane without addition of TiO₂. P25-TiO₂ powder is a mixture of two different forms of TiO₂, i.e. anatase (75%) (JCPDS card No. 21–1272) and rutile (25%) (JCPDS card No. 34–180)

Table 2
Effect of TiO₂ concentration on the PVDF membrane properties with respect to porosity, mechanical strength, contact angle and pore size

TiO ₂ concentration (wt.%)	Porosity (%)	Tensile strength (MPa)	Contact angle (°)	Pore size (nm)
0	86.8	1.94	74.9	98.2
1	87.5	2.55	73.8	100.9
2	88.6	2.58	68.4	104.4
3	84.1	2.43	74.3	102.8
4	87.6	2.42	75.7	94.3

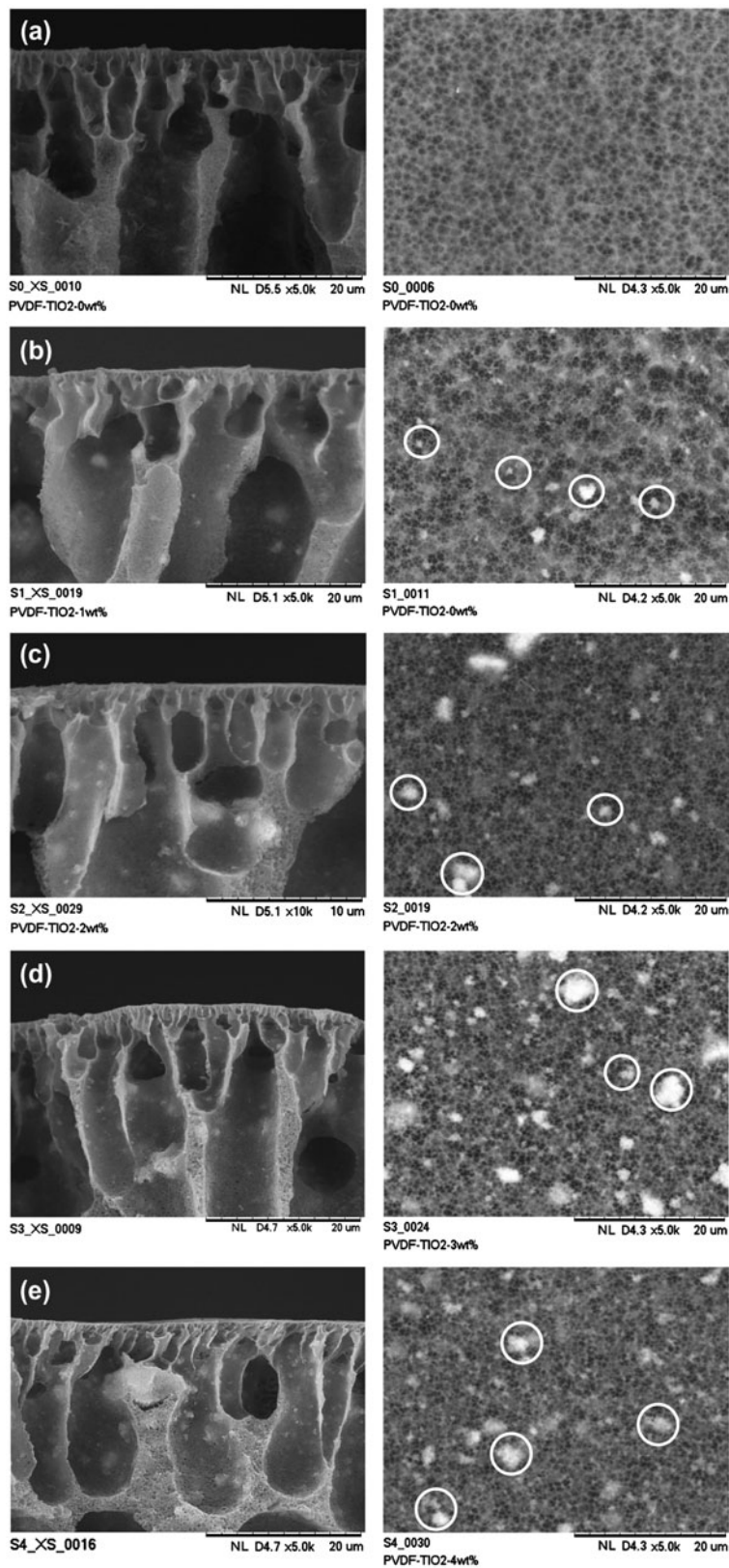


Fig. 2. SEM images (cross-section and outer surface) of PVDF membranes prepared from different TiO₂ concentrations, (a) 0 wt.%, (b) 1 wt.%, (c) 2 wt.%, (d) 3 wt.% and (e) 4 wt.%, in the presence of hydrophilic PVP.

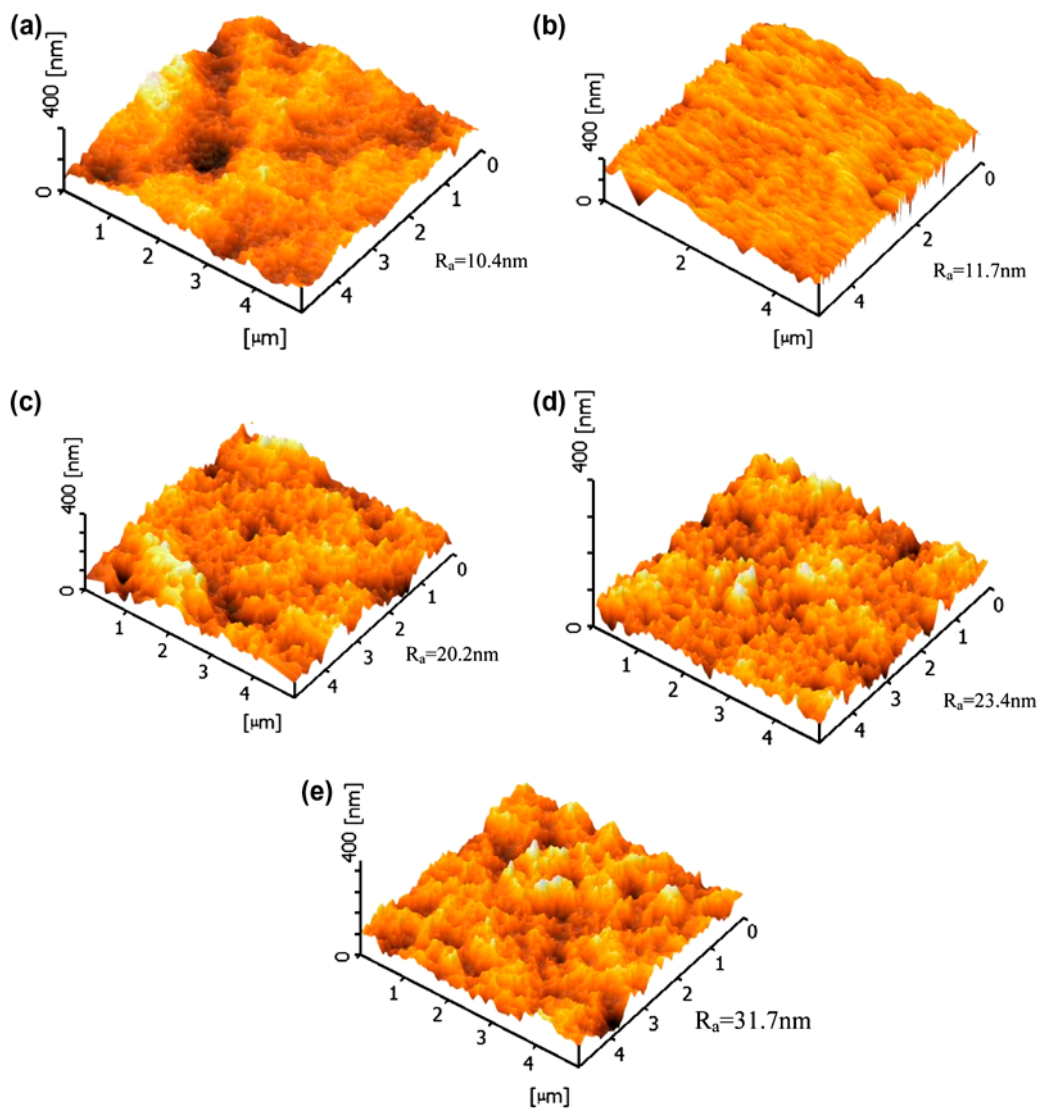


Fig. 3. 3D AFM images of PVDF membranes prepared from different TiO_2 concentrations, (a) 0 wt.%, (b) 1 wt.%, (c) 2 wt.%, (d) 3 wt.% and (e) 4 wt.%, in the presence of hydrophilic PVP.

[26]. As can be seen from Fig. 5, there are three dominant peaks at 2θ of 25.4° , 37.9° , and 48.45° , which are analogous with the characteristic peaks of P25- TiO_2 crystal powder [21]. The presence of these three significant peaks for PVDF- TiO_2 membranes compared to PVDF membrane indicated that TiO_2 nanoparticles were uniformly distributed in the hollow fiber membrane prepared from phase inversion process.

3.2. Effect of TiO_2 concentration on membrane flux and oil rejection

Fig. 6 shows the effect of TiO_2 concentration on PVDF membrane performances in treating synthesized

oily solution of 250 ppm oil concentration. The tendency of membrane water flux change was identical to that of pure water flux change, where the PVDF membrane with 2 wt.% TiO_2 concentration displayed the highest water flux, while the PVDF membrane without addition of TiO_2 demonstrated the lowest. As can be seen from Fig. 6(a), the pure water flux of PVDF membrane was increased from 32.50 to 75.68 $\text{L}/\text{m}^2\text{h}$ with increasing TiO_2 concentration from 0 to 2 wt.%, exhibiting more than 130% enhancement in water permeability. This significant improvement can be mainly attributed to the increased membrane hydrophilicity coupled with the increase in membrane pore dimension upon the addition of highly

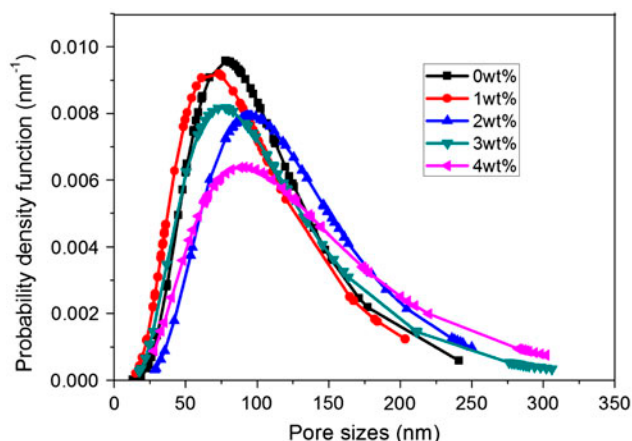


Fig. 4. Probability density function curve generated from the pore sizes measured by AFM for PVDF membrane prepared at different TiO₂ concentration.

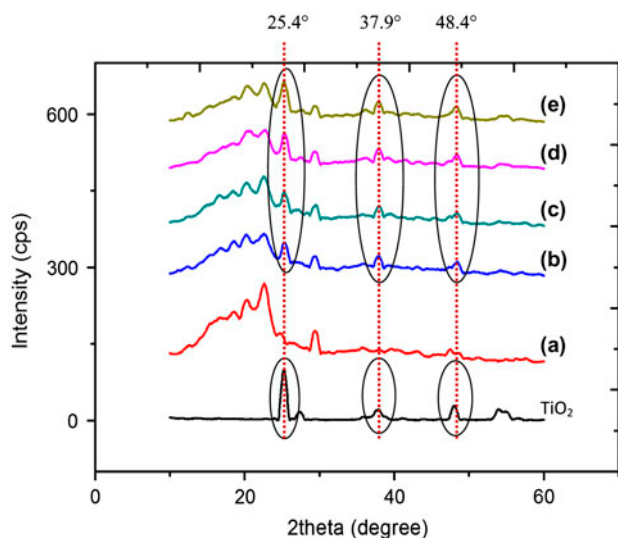


Fig. 5. XRD graph of P25-TiO₂ and PVDF membrane prepared at different TiO₂ concentration, (a) 0 wt.%, (b) 1 wt.%, (c) 2 wt.%, (d) 3 wt.% and (e) 4 wt.%.

hydrophilic inorganic additive. Further increase in TiO₂ concentration to 3 and 4 wt.%, however, resulted in water flux reduction as membrane pore size was decreased from 104.4 nm, as reported in the membrane incorporated with 2 wt.% TiO₂ to 102.8 and 94.3 nm as evidenced in the membrane with 3 and 4 wt.% TiO₂, respectively. The decrease in pore size of the membranes prepared at high concentration of TiO₂ was mainly attributed to the pore blocking caused by agglomeration of TiO₂ on membrane surface (see Fig. 2(d) and (e)). Besides blocking membrane pores, the agglomeration of TiO₂ nanoparticles is also able to reduce the contact area of hydroxyl groups carried by

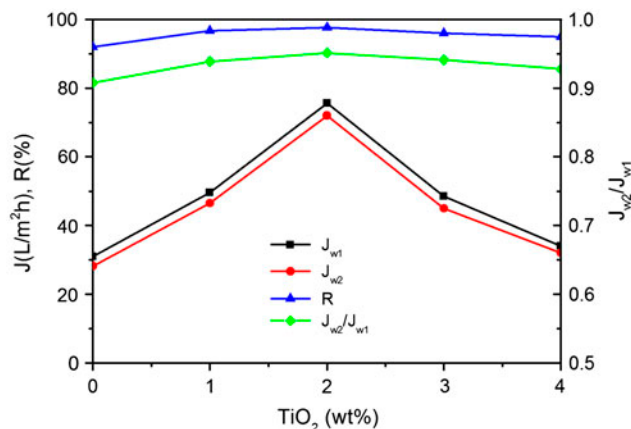


Fig. 6. (a) Pure water flux (J_{w1}), permeate flux (J_{w2}) and rejection (%) (b) ratio of J_{w2}/J_{w1} of PVDF membranes prepared at different TiO₂ concentration (operating conditions: temperature = 25°C, oil concentration = 250 ppm, air bubble flow rate = 5 mL/min and vacuum pressure = -15 in Hg).

TiO₂ nanoparticles with water molecules, which further affect membrane water permeation rate. As has been evidenced by other researchers as well [14,21,27], overloading of TiO₂ could adversely affect the membrane properties mainly due to the nonuniform dispersion of nanoparticles on membrane surface that caused severe TiO₂ agglomeration.

For the oily wastewater treatment experiments, it is found that the water flux of the PVDF membrane without addition of TiO₂ was decreased from initial value of 31.0 (tested using pure water) to <28.0 L/m²h in oily solution, while PVDF membrane with 2 wt.% TiO₂ displayed 72.0 L/m²h water flux compared to 76.0 L/m²h when tested using pure water. This phenomenon is common as the presence of oil molecules in the feed solution might accumulate on the membrane surface, hence creating additional transport resistance for water to permeate and leading to reduction in water flux as evidenced in this study. With respect to oil rejection, it is found that all membranes demonstrated very promising rejection performance, where at least 90% of oil removal was achieved. It is thus believed that the mean pore size of membranes (see Table 2) is small enough to separate bigger emulsified oil from oily solution. The average oil particle size from the synthetic oily wastewater was reported to be around 1.08 μm as shown in Fig. 1, which is much bigger than the pore size of the membrane studied in this work. By taking into the account water flux and oil rejection, it is concluded that PVDF membrane prepared from 2 wt.% TiO₂ nanoparticles was the optimum membrane, as it achieved the highest water flux and excellent oil rejection greater than 97%.

The antifouling properties of PVDF–TiO₂ composite membranes were evaluated based on the ratio of permeate flux (J_{w2}) and pure water flux (J_{w1}). It was found that all PVDF–TiO₂ composite membranes demonstrated higher water flux ratio than that of PVDF membrane without addition of TiO₂, indicating that the addition of TiO₂ has increased the antifouling properties of the composite PVDF membrane. It can be explained by the antifouling properties of TiO₂, reducing the accumulation of oil particles on the membrane surface and resulted in the higher water flux ratio (J_{w2}/J_{w1}). Fig. 6 also shows that the water flux ratio was maximum with 2 wt.% TiO₂. This can be explained by the fact that the high hydrophilicity of this membrane has effectively reduced the interaction between the hydrophobic oily particles and membrane surface, hence resulting in excellent antifouling properties.

3.3. Effect of oil concentration on optimum membrane flux and oil rejection

The separation performance of the optimum membrane was further investigated using feed oily solution with concentration ranging from 250 to 1,000 ppm. The normalized water flux and oil rejection of membrane as a function of time are shown in Fig. 7. By comparing the performance of membrane tested under different feed concentrations, it was found that at lower oil concentration, the membrane flux decline was not as severe as that observed at high concentration. For 250 ppm oily solution, the membrane was reported to decline around 29% after 3 h operation compared to 42 and 34% reported for 500 and 1,000 ppm oily solution, respectively. The increase in flux decline rate with increasing oil concentration can be explained by the formation of denser/thicker oil layer on the membrane outer surface, which has led to the increase in water transport resistance. Based on the results obtained, it can be deduced that the good antifouling property of composite membrane was compromised when it was tested using high concentration of oily solution (i.e. 1,000 ppm). Even though the hydrophilic nature of PVDF membrane has been enhanced upon the addition of two hydrophilic additives (i.e. TiO₂ and PVP), the presence of significant amount of oil molecules in the feed solution was found to unfavorably cover the membrane surface, hence reduced its hydrophilicity. Nevertheless, the composite membranes prepared in this study can be sufficiently used to treat the oily solution discharged from industries without experiencing severe flux decline as the oil concentration of industrial effluent normally falls in the range of 100–450 ppm [6,28–30].

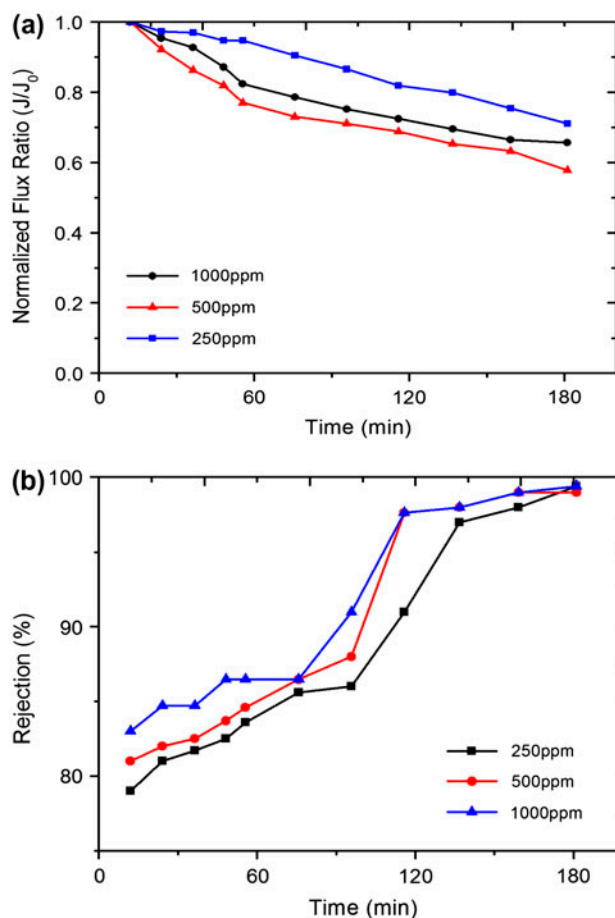


Fig. 7. Performance of PVDF membrane incorporated with optimized 2 wt.% TiO₂ at different oil concentrations, (a) normalized flux ratio and (b) oil rejection.

Despite the decline in membrane flux, improved oil separation was observed with the increasing feed oil concentration. This can be explained by the fact that the formation of oil layer could act as an additional selective layer to the membrane barrier to improve the oil rejection. At 250 ppm, the initial oil rejection was around 78%, but it was slowly increased with time and eventually achieved almost complete removal of oil after 3 h. Compared with 500 and 1,000 ppm oily solution, there was slightly difference in oil rejection at the early stage of the operation, but very similar separation behavior was observed towards the end of experiment.

4. Conclusions

PVDF hollow fiber membranes with different TiO₂ concentrations were successfully prepared and their oil separation performances were evaluated using oily solution of different concentrations. Results revealed

that the addition of 2 wt.% TiO₂ nanoparticles concentration in PVDF membrane played a significant role in improving membrane properties by increasing membrane hydrophilicity, pore size, and surface roughness. Higher concentration of TiO₂ has led to the deterioration of membrane performance due to agglomeration of nanoparticles on membrane surface. The high membrane porosity obtained at various concentrations of TiO₂ was due to the presence of PVP in the membrane dope. PVDF membrane with 2 wt.% TiO₂ showed 70.48 L/m²h of water flux and 99.7% of oil rejection when tested using 250 ppm oily solution under vacuum condition. Although increasing feed oil concentration from 250 to 1,000 ppm resulted in membrane-declined water flux, the oil separation rate was improved mainly due to the additional selective layer formed by oil layer on membrane surface. Overall, it can be concluded that the PVDF composite membrane prepared in this work could be potentially used to treat oily wastewater discharged from industry.

References

- [1] M.H. El-Naas, S. Al-Zuhair, A. Al-Lobaney, S. Makhlof, Assessment of electrocoagulation for the treatment of petroleum refinery wastewater, *J. Environ. Manage.* 91 (2009) 180–185.
- [2] S. Shokrollahzadeh, F. Golmohammad, N. Naseri, H. Shokouhi, M. Arman-mehr, Chemical oxidation for removal of hydrocarbons from gas-field produced water, *Procedia Eng.* 42 (2012) 942–947.
- [3] A.F. Viero, T.M. de Melo, A.P.R. Torres, N.R. Ferreira, G.L. Sant'Anna Jr., C.P. Borges, V.M.J. Santiago, The effects of long-term feeding of high organic loading in a submerged membrane bioreactor treating oil refinery wastewater, *J. Membr. Sci.* 319 (2008) 223–230.
- [4] M.H. El-Naas, S. Al-Zuhair, M.A. Alhaija, Reduction of COD in refinery wastewater through adsorption on date-pit activated carbon, *J. Hazard. Mater.* 173 (2010) 750–757.
- [5] L. Zhidong, L. Na, Z. Honglin, L. Dan, Study of an A/O submerged membrane bioreactor for oil refinery wastewater treatment, *Pet. Sci. Technol.* 27 (2009) 1274–1285.
- [6] B. Chakrabarty, A.K. Ghoshal, M.K. Purkait, Cross-flow ultrafiltration of stable oil-in-water emulsion using polysulfone membranes, *Chem. Eng. J.* 165 (2010) 447–456.
- [7] Y. Pan, T. Wang, H. Sun, W. Wang, Preparation and application of titanium dioxide dynamic membranes in microfiltration of oil-in-water emulsions, *Sep. Purif. Technol.* 89 (2012) 78–83.
- [8] A. Zirehpour, M. Jahanshahi, A. Rahimpour, Unique membrane process integration for olive oil mill wastewater purification, *Sep. Purif. Technol.* 96 (2012) 124–131.
- [9] B. Chakrabarty, A.K. Ghoshal, M.K. Purkait, Preparation, characterization and performance studies of polysulfone membranes using PVP as an additive, *J. Membr. Sci.* 315 (2008) 36–47.
- [10] Z. Yuan, X. Dan-Li, Porous PVDF/TPU blends asymmetric hollow fiber membranes prepared with the use of hydrophilic additive PVP (K30), *Desalination* 223 (2008) 438–447.
- [11] Z.L. Xu, T.S. Chung, Y. Huang, Effect of polyvinylpyrrolidone molecular weights on morphology, oil/water separation, mechanical and thermal properties of polyetherimide/polyvinylpyrrolidone hollow fiber membranes, *J. Appl. Polym. Sci.* 74 (1999) 2220–2233.
- [12] A. Rahimpour, M. Jahanshahi, A. Mollahosseini, B. Rajaeian, Structural and performance properties of UV-assisted TiO₂ deposited nano-composite PVDF/SPES membranes, *Desalination* 285 (2012) 31–38.
- [13] S.J. Oh, N. Kim, Y.T. Lee, Preparation and characterization of PVDF/TiO₂ organic-inorganic composite membranes for fouling resistance improvement, *J. Membr. Sci.* 345 (2009) 13–20.
- [14] R.A. Damodar, S.J. You, H.H. Chou, Study the self cleaning, antibacterial and photocatalytic properties of TiO₂ entrapped PVDF membranes, *J. Hazard. Mater.* 172 (2009) 1321–1328.
- [15] A. Rahimpour, M. Jahanshahi, B. Rajaeian, M. Rahimnejad, TiO₂ entrapped nano-composite PVDF/SPES membranes: Preparation, characterization, antifouling and antibacterial properties, *Desalination* 278 (2011) 343–353.
- [16] W.J. Lau, A.F. Ismail, Theoretical studies on the morphological and electrical properties of blended PES/SPEEK nanofiltration membranes using different sulfonation degree of SPEEK, *J. Membr. Sci.* 334 (2009) 30–42.
- [17] M. Khayet, C.Y. Feng, K.C. Khulbe, T. Matsuura, Preparation and characterization of polyvinylidene fluoride hollow fiber membranes for ultrafiltration, *Polymer* 43 (2002) 3879–3890.
- [18] Y. Yang, H. Zhang, P. Wang, Q. Zheng, J. Li, The influence of nano-sized TiO₂ fillers on the morphologies and properties of PSF UF membrane, *J. Membr. Sci.* 288 (2007) 231–238.
- [19] H.L. Feng, X.Z. Liang, Y.L. Yun, W.Y. Ming, C. Yue, Performance of PVDF/multi-nanoparticles composite hollow fibre ultrafiltration membranes, *Iran. Polym. J.* 19 (2010) 553–565.
- [20] F. Shi, Y. Ma, J. Ma, P. Wang, W. Sun, Preparation and characterization of PVDF/TiO₂ hybrid membranes with different dosage of nano-TiO₂, *J. Membr. Sci.* 389 (2012) 522–531.
- [21] L.Y. Yu, H.M. Shen, Z.L. Xu, PVDF-TiO₂ composite hollow fiber ultrafiltration membranes prepared by TiO₂ sol-gel method and blending method, *J. Appl. Polym. Sci.* 113 (2009) 1763–1772.
- [22] S. Majeed, D. Fierro, K. Buhr, J. Wind, B. Du, A. Boschetti-de-Fierro, V. Abetz, Multi-walled carbon nanotubes (MWCNTs) mixed polyacrylonitrile (PAN) ultrafiltration membranes, *J. Membr. Sci.* 403–404 (2012) 101–109.
- [23] R. Jamshidi Gohari, W.J. Lau, T. Matsuura, A.F. Ismail, Effect of surface pattern formation on membrane fouling and its control in phase inversion process, *J. Membr. Sci.* 446 (2013) 326–331.
- [24] S. Singh, K.C. Khulbe, T. Matsuura, P. Ramamurthy, Membrane characterization by solute transport and

- atomic force microscopy, *J. Membr. Sci.* 142 (1998) 111–127.
- [25] C.Y. Feng, K.C. Khulbe, G. Chowdhury, T. Matsuura, V.C. Sapkal, Structural and performance study of microporous polyetherimide hollow fiber membranes made by solvent-spinning method, *J. Membr. Sci.* 189 (2001) 193–203.
- [26] B. Zielińska, E. Borowiak-Palen, R.J. Kalenczuk, A study on the synthesis, characterization and photocatalytic activity of TiO₂ derived nanostructures, *Mater. Sci.* 28 (2010) 625–637.
- [27] E. Yuliwati, A.F. Ismail, T. Matsuura, M.A. Kassim, M.S. Abdullah, Characterization of surface-modified porous PVDF hollow fibers for refinery wastewater treatment using microscopic observation, *Desalination* 283 (2011) 206–213.
- [28] M. Ebrahimi, K.S. Ashaghi, L. Engel, D. Willershausen, P. Mund, P. Bolduan, P. Czermak, Characterization and application of different ceramic membranes for the oil-field produced water treatment, *Desalination* 245 (2009) 533–540.
- [29] R. Šećerov Sokolović, S. Sokolović, S. Šević, Oily water treatment using a new steady-state fiber-bed coalescer, *J. Hazard. Mater.* 162 (2009) 410–415.
- [30] M. Gryta, K. Karakulski, A.W. Morawski, Purification of oily wastewater by hybrid UF/MD, *Water Res.* 35 (2001) 3665–3669.